$J/\psi \to \mu^+\mu^-$ reconstruction in the CMS experiment*

YANG Zong-Chang(杨宗长) QIAN Si-Jin(钱思进)[1)]

(State Key Laboratory of Nuclear Science and Technology, Peking University, Beijing 100871, China)

Abstract In this paper the $J/\psi \to \mu^+\mu^-$ reconstruction performance in the CMS experiment at the LHC is studied in detail by using $B_s \to J/\psi\,\phi \to \mu\mu KK$ events. The reconstruction efficiencies of J/ψ mesons and their decay muons are obtained as a function of the transverse momentum p_T and the pseudo-rapidity η. We also study the muon trigger efficiency for this channel with the planned Level-1 trigger and High Level Trigger selection criteria. It was observed that the muon reconstruction efficiency decreases when the two decay muons have a small or large 3D angular separation, which further affects the overall J/ψ reconstruction efficiency.

Key words CMS, J/ψ, reconstruction efficiency, Level-1 trigger, HLT (High Level Trigger)

PACS 13.25.Gv

1 Introduction

The Large Hadron Collider (LHC) built at the European Organization for Nuclear Research (CERN) near Geneva, Switzerland across the Swiss-French border was planned to start operations in the autumn of 2008 after more than 10 years of construction. LHC[1] will be the most powerful particle accelerator in the world with the head-on collisions of two proton beams of up to 7 TeV of energy per beam, which is 7 times higher than the current world record held by the Tevatron at Fermilab near Chicago in USA. The LHC will also provide the most intense beams, reaching a luminosity of up to 10^{34} $cm^{-2}\cdot s^{-1}$ or higher. These new frontiers of energy and luminosity will give us a powerful tool to explore the important TeV scale physics, including the searches for Higgs bosons, supersymmetric particles, extra dimensions as well as the extended regions in standard model physics, etc.

The Compact Muon Solenoid (CMS)[2] is one of the two large general purpose experiments at LHC. The detector has a cylindrical shape with dimensions of 15 m in diameter and 21.5 m in length; its total weight is about 12500 ton. The CMS detector has five major sub-systems which are, starting from the interaction point of beam collision along the axial line of the detector outwards, (1) the silicon tracker (including the silicon pixel and strips), (2) the electro-magnetic calorimeter (ECAL), (3) the hadron calorimeter (HCAL), (4) the superconducting solenoid with a magnetic field of 3.8 T, and (5) the muon system which includes the Drift Tube (DT) chambers in the barrel, the Cathode Strip Chamber (CSC) in the endcap, and a Resistive Plate Chamber (RPC) in both the barrel and endcap regions.

This study has mainly used the robust CMS muon and tracker systems which have large acceptances (pseudo-rapidity $|\eta| < 2.5$ and full azimuthal angular coverage of 2π) and excellent resolutions. The hadrons have been absorbed in ECAL, HCAL and the magnet's yoke before reaching the Muon chambers, so the background of muon detection can be minimized. However, due to the large diameter and the strong field of the solenoid magnet as well as the energy loss between the interaction point and the first muon chamber, the muons with low transverse momentum (p_T) cannot reach the muon chambers, thus CMS has no sensitivity for low p_T (<3 GeV/c) muons.

Our initial physics motivation is to study the production mechanism and polarization of J/ψ mesons in the high-p_T region[3]. The J/ψ production rate calculated by the leading order Color Singlet Model of Non-Relativistic QCD (NRQCD) is lower by a couple of orders of magnitude than the rate measured by the

Received 6 August 2008

* Supported by NSFC (10435070, 10099630) and Ministry of Science and Technology of China (2007CB816101)

1) E-mail: sijin.qian@cern.ch

CDF experiment at the Tevatron, while the Color Octet Mechanism (COM) may help NRQCD to fit the CDF data[4]. However, the predictions of COM on J/ψ polarization still disagree with the experimental data from the Tevatron experiments[5]. In the light of this so-called "polarization puzzle" and the large yield of J/ψ mesons produced at the LHC, the early data collected by CMS seems to provide an ideal opportunity to extend the test of different J/ψ production mechanisms to higher p_T regions than are feasible at Tevatron experiments. Unfortunately, at the time of this study, no datasets were available with properly simulated COM processes, thus we used those available Monte-Carlo datasets to study the J/ψ reconstruction first.

Events containing J/ψ mesons are of interest for several other topics in B-physics and heavy-ion physics. They can also be used for calibration purposes, and the reconstruction of the mass resonance in their di-muon decay mode will be a fundamental tool to check the scale of the reconstructed muon momentum. The present study aims to provide useful information for all topics related to J/ψ mesons in the CMS.

We used a sample of simulated $B_s \rightarrow J/\psi$ events to study the muon and J/ψ reconstruction efficiencies as a function of p_T or η in di-muon events, as well as their dependence on the 3D angular separation between the two decayed muons. Potential differences in performance between the barrel region (i.e. the Drift Tube (DT) muon subsystem) and the end-cap region (i.e. the Cathode Strip Chamber (CSC) muon subsystem) were also addressed. Finally, the influence of the trigger selection on the J/ψ acceptance was quantified.

In this paper, the B_s data sample and its statistics are described in Section 2. The reconstruction of di-muons and of J/ψ mesons is explained in Sections 3 and 4, respectively. Section 5 illustrates the efficiency dependence on the angular separation between the two decay muons. Section 6 contains the result of studying the trigger selection. Some conclusions are drawn in Section 7.

2 Data sample used in the analysis

The $B_s \rightarrow J/\psi\phi \rightarrow \mu\mu KK$ events were generated with the CMS kinematics package CMKIN version 1.0.1 (Pythia 6.223)[6], simulated with the CMS simulation package OSCAR version 2.4.5 (MagneticField: CMSIMField)[7] and digitized with low luminosity pileup using the CMS reconstruction package ORCA version 8.6.1. The Data Summary Tapes production was done with the ORCA version 8.7.1 package[8].

This dataset contains 198725 events at the generator level, and a total 432272 muons in 192500 events with pre-selection: at least one muon $|\eta| < 2.4$. The p_T and η distributions of muons are shown in Fig. 1.

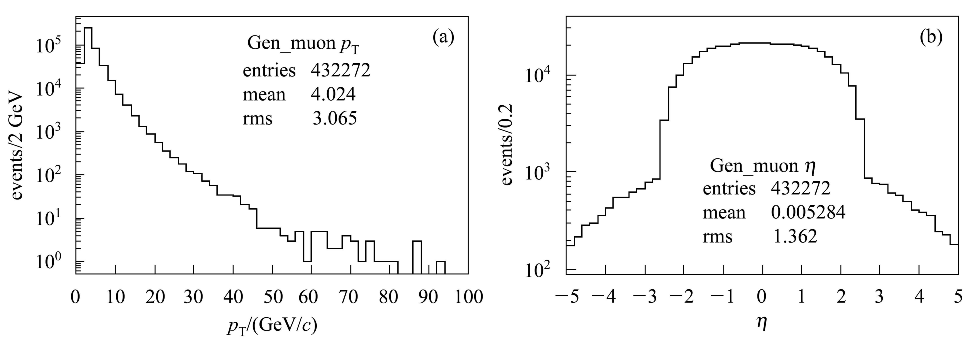

Fig. 1. (a) p_T and (b) η distributions of muons (at generator level).

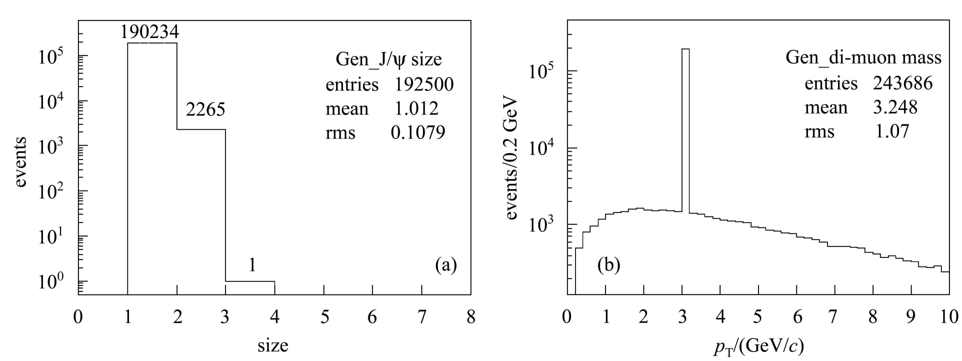

Fig. 2. (a) Number of J/ψ mesons per event and (b) di-muon invariant mass distribution (at generator level).

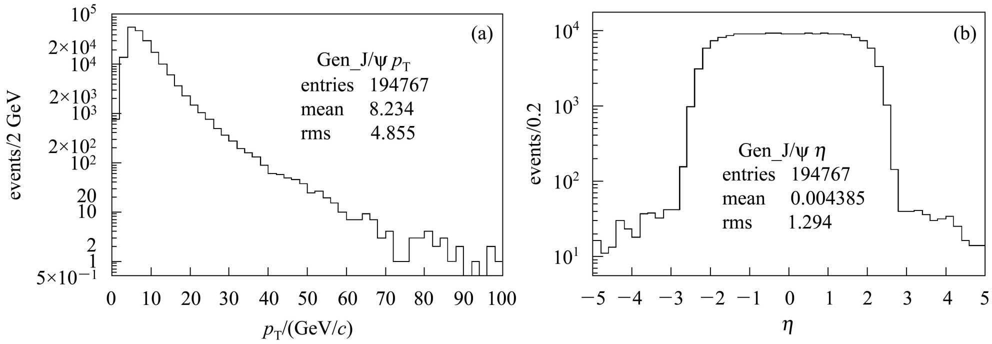

Fig. 3. (a) p_T and (b) η distributions of the J/ψ mesons (at generator level).

All the events in this dataset contain at least one J/ψ, but some events have more than one J/ψ, as shown in Fig. 2(a). The J/ψ coming from the B_s was forced to decay into two muons, but the extra J/ψ mesons in the event were not forced to do so. Therefore we will normalize reconstruction efficiencies according to the number of generated di-muons within a mass window (from 2.95 to 3.25 GeV/c^2) instead of using the total number of J/ψ mesons at generator level. Fig. 2(b) shows the distribution of the di-muon invariant mass. It should be noted that some muon pairs include muons not coming from the B_s decay. In addition, all possible pairings are considered if there are more than two muons in the event. Fig. 3 shows the p_T and η distributions of all J/ψ mesons.

3 Muon reconstruction

There are 118059 muons reconstructed by the global muon reconstructor of ORCA[8] in the B_s dataset. The p_T and η distributions of these reconstructed muons are shown in Fig. 4. Comparing Fig. 4(b) with Fig. 1(b), it can be seen that almost all muons with $|\eta|$ >2.4 (which is the acceptance of the CMS muon system) are not reconstructed.

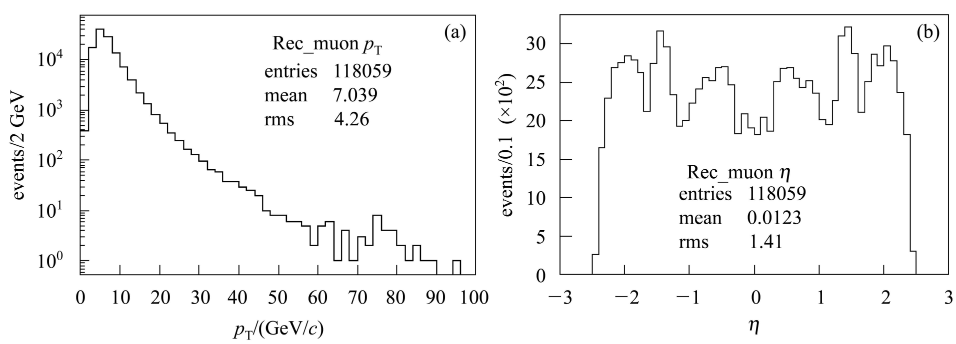

Fig. 4. (a) p_T and (b) η distributions of reconstructed muons.

3.1 Matching of reconstructed and simulated muons

The reconstructed muons are matched with the muons at generator level via kinematic cuts. In the same event, we compare the charges, momenta and directions of the muons. A muon-1 at the generator level, with a momentum p_1, a polar angle θ_1 and an azimuthal angle Φ_1, is declared to be matched with a muon-2 at reconstruction level, with a momentum of p_2 and angles θ_2 and Φ_2, if:

(1) charge of muon-1 = charge of muon-2

(2) $|1/p_1 - 1/p_2| < 10\Delta(1/p)$

(3) $|\theta_1 - \theta_2| < 10\Delta\theta$

(4) $|\Phi_1 - \Phi_2| < 10\Delta\Phi$,

where $\Delta(1/p)$, $\Delta\theta$ and $\Delta\Phi$ are the errors provided by the muon reconstruction fit. They represent the resolutions on the parameters $1/p$, θ and Φ. A typical value of $\Delta p/p$ is 1.5%.

There are 113148 reconstructed muons matched and 4907 reconstructed muons unmatched to their generated counterparts. The remaining difference (4 muons) between the sum of these two numbers and the number of entries in Fig. 4(a) is due to events where two muons are too close: they are counted as just one muon after matching. Fig. 5 shows the p_T

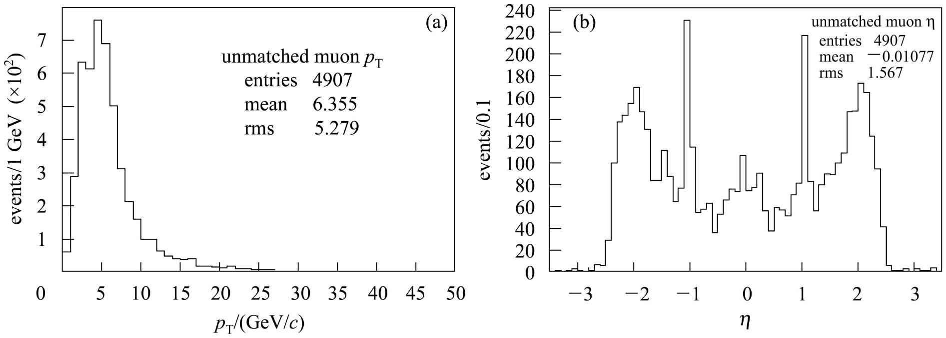

Fig. 5. (a) p_T and (b) η distributions of unmatched muons.

and η distributions of the unmatched muons, where it can be seen that most of the unmatched muons are at p_T <10 GeV/c and $|\eta|$ >1.0, and are due to the second condition, i.e. p unmatched. From Fig. 5(b), we can see two peaks at $|\eta|$ ~0.9—1.2, where the barrel to end-cap transition occurs.

3.2 Muon reconstruction efficiency

The single muon reconstruction performance in the CMS was described in Ref. [9]. Here we define the reconstruction efficiency in the case of di-muons as $\varepsilon_{\text{muon}} = \dfrac{N_{\text{recmuon}}}{N_{\text{genmuon}}}$, with: N_{genmuon}: the number of muons considered at generator level with some cuts, e.g. $|\eta|$ <2.4 for Fig. 6(a) or p_T >5 GeV/c for Fig. 6(b); N_{recmuon}: the number of muons correctly matched with the muons in N_{genmuon}. This efficiency will be a little lower than the single muon efficiency due to the matching criteria described in Sect. 3.1.

The efficiency for reconstruction of the decayed muons in this B_s sample is shown in Fig. 6(a) as a function of p_T for muons with $|\eta|$ <2.4 and in Fig. 6(b) as a function of η for muons with different p_T.

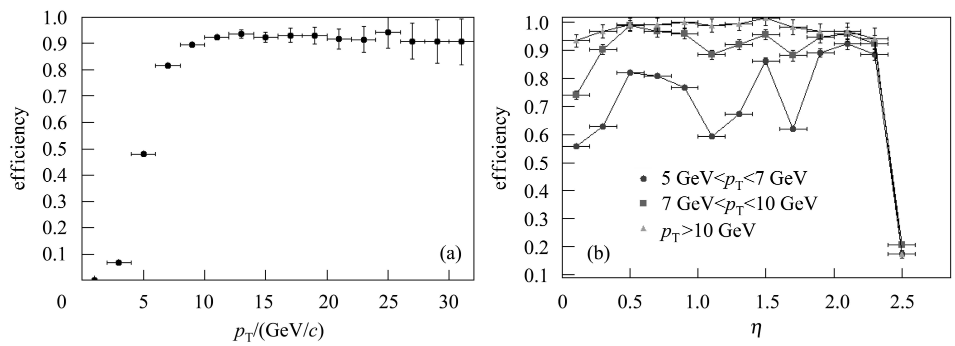

Fig. 6. Muon reconstruction efficiency vs. p_T (a), and vs. η (b).

From Fig. 6(a), it can be seen that the efficiency is above 90% for muons with p_T >9 GeV/c. Many low p_T muons have very low efficiency because they hardly reach the muon system. There are three curves in Fig. 6(b), corresponding to muons in different p_T regions. Two drops can be seen around $|\eta|$ ~1.1 and ~1.7, which are more significant for low p_T muons.

4 J/ψ reconstruction

4.1 Invariant mass and mass resolution of reconstructed J/ψ mesons

J/ψ mesons are reconstructed by considering all pairs of oppositely charged muons in an event and constructing their invariant mass. Any di-muon with an invariant mass in the mass window (2.95—3.25 GeV/c^2) is considered as a J/ψ candidate. The reconstructed J/ψ mass peak can be fit nicely with a Gaussian function[10]. The p_T and η distributions of reconstructed J/ψ mesons are shown in Fig. 7.

There are 19971 J/ψ mesons reconstructed with an overall J/ψ reconstruction efficiency of about 10.1%. The mean of the reconstructed J/ψ mass is 3.11 GeV/c^2 and the mass resolution is about 34 MeV/c^2 (i.e. ~1.1%).

4.2 J/ψ reconstruction efficiency

The J/ψ reconstruction efficiency is defined as $\varepsilon_{\text{Jpsi}} = \dfrac{N_{\text{recJpsi}}}{N_{\text{genJpsi}}}$, with: N_{genJpsi}: the number of di-muons at generator level within the reference invariant mass window (2.95—3.25 GeV/c^2), and with some cuts (as indicated below and in the legend of Fig. 8(b)) on the p_{T} or η of the muons; N_{recJpsi}: the number of di-muons at reconstruction level within the reference invariant mass window (2.95—3.25 GeV/c^2). The J/ψ reconstruction efficiencies as a function of the p_{T} and η of the J/ψ are shown in Fig. 8. The cut $|\eta|$ <2.4 has been applied to both muons.

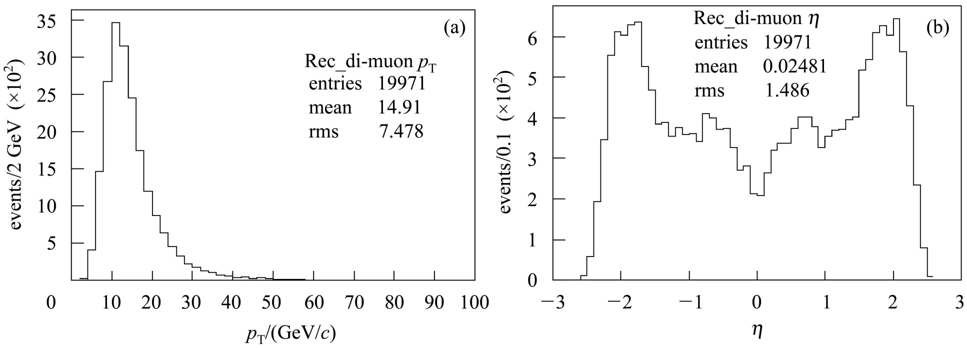

Fig. 7. (a) p_{T} and (b) η distributions of reconstructed J/ψ mesons.

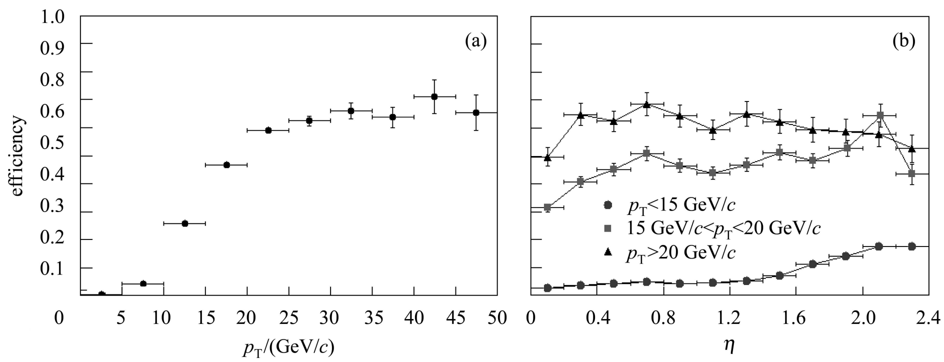

Fig. 8. J/ψ reconstruction efficiency vs. generated p_{T} (a), and vs. generated η (b).

These efficiencies do not take into account the trigger acceptance. The J/ψ efficiency under different trigger conditions will be discussed in Section 6.

From Fig. 8, it can be seen that the offline J/ψ reconstruction efficiency can reach 60%—70% for p_{T} of the J/ψ meson above 25 GeV/c; the dependence of the efficiency on η is moderate for J/ψ mesons with higher p_{T}, but is quite dramatic for J/ψ mesons with lower p_{T} (e.g. below 20 GeV/c).

5 Dependence of the J/ψ reconstruction efficiency on the separation angle between muons

It was reported[11] by another LHC experiment that the efficiency for reconstructing di-muons from J/ψ decays is dependent upon the angular separation between the two muons in their detector. We have tried to verify whether this would be detector-specific or not.

The 3D angular separation $\Delta\Omega_{\mu\mu}$ between two decay muons in the laboratory frame is determined from the expression: $\cos\Delta\Omega_{\mu\mu}= (p^2-p_1^2-p_2^2)/(2p_1p_2)$, where p_1 and p_2 are the muon momenta and p is the momentum of the J/ψ(→ μμ) system, all in the laboratory frame.

Figure 9 shows the di-muon reconstruction efficiency as a function of this angular separation, where both muons are required to have p_{T} >6 GeV/c and $|\eta|$ <2.4 at generation level.

It is observed that the di-muon reconstruction efficiency is degraded when the two muons have a small 3D angular separation (i.e. $\Delta\Omega_{\mu\mu} < 0.05$ radians) or a large one (i.e. $\Delta\Omega_{\mu\mu} > 0.4$ radians). The efficiency drop at small separation angles is more significant in the endcap region (i.e. CSCs), likely due to ghost segments created when both muons traverse the same CSC chamber.

In order to understand the efficiency drop at large separation angles, the $|\eta|$ and p_{T} distributions of di-muons with different 3D separation angles $\Delta\Omega_{\mu\mu}$ are shown in Figs. 10 and 11. Both muons are required to satisfy the generator level conditions mentioned above and used in Fig. 9.

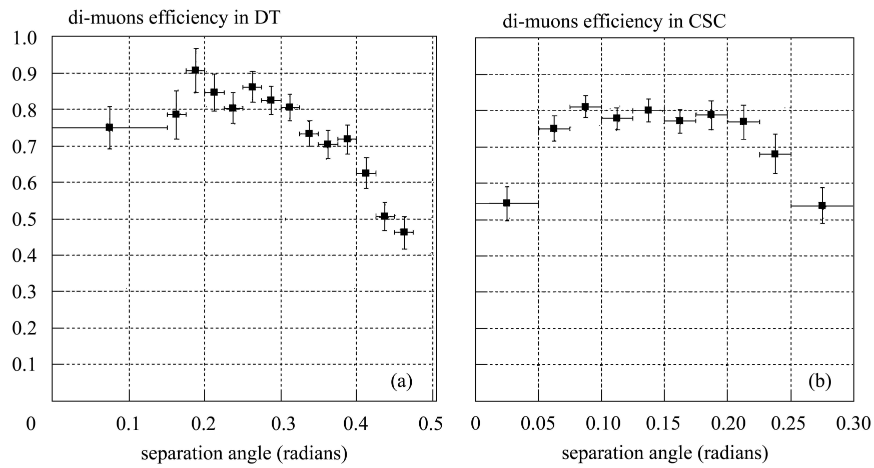

Fig. 9. Reconstruction efficiency of di-muons from J/ψ decays vs. their angular separation in the barrel region ($|\eta|<1.0$), mainly covered by DTs (a), and in the endcap region ($|\eta|>1.0$), mainly covered by CSCs (b).

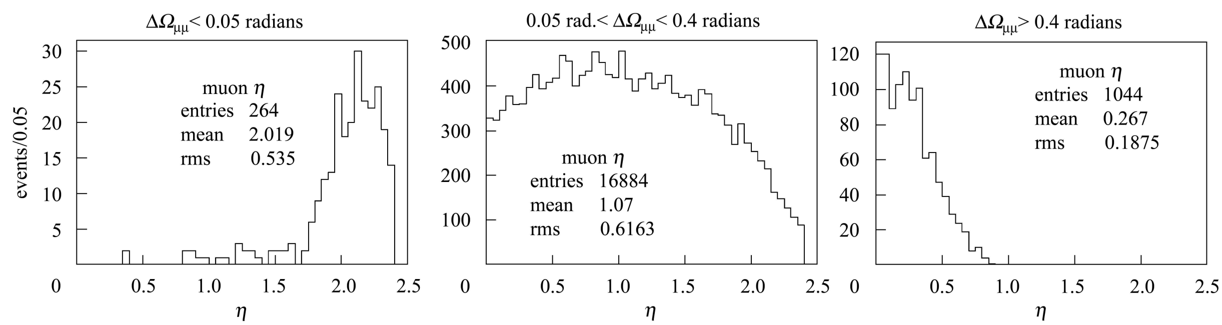

Fig. 10. The $|\eta|$ distribution of the di-muons for different separation angles.

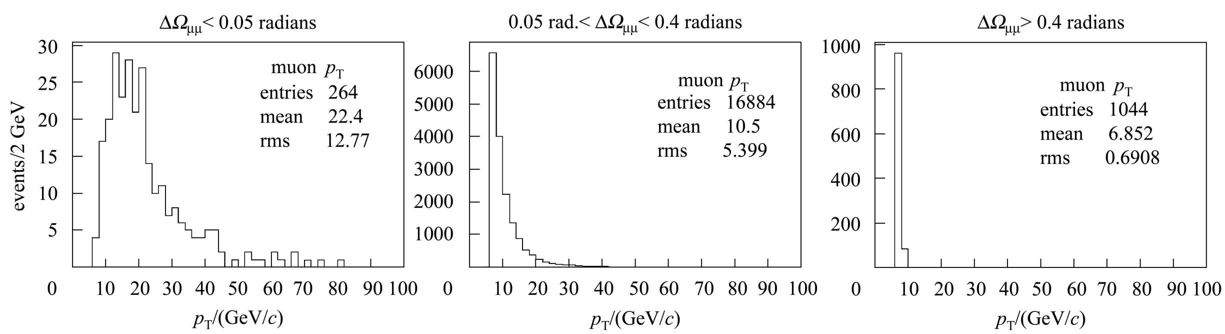

Fig. 11. The p_{T} distributions of the di-muons for different separation angles.

From the right plot of Fig. 11 it can be seen that, for the $\Delta\Omega_{\mu\mu}>0.4$ radians case, all muons have $p_{\mathrm{T}}<10$ GeV/c, which causes a decrease of efficiency according to Fig. 6. From the left plot of Fig. 10, we also can cross-prove that, as mentioned above for the case of $\Delta\Omega_{\mu\mu}<0.05$ radians, most muons have high $|\eta|$ (i.e. are in the endcap CSC region). This is kinematically enforced because to get a 3.1 GeV/c^2 invariant mass with a small separation angle requires large momenta, which are more frequent at high $|\eta|$.

Therefore, a summary may be made as a reference for the future J/ψ studies in CMS:

(1) the efficiency drop at small separation angles is mainly due to the presence of muons in high $|\eta|$ (i.e. CSC) region;

(2) the efficiency drop at large separation angles is due to the presence of low p_{T} muons.

6 Trigger analysis

6.1 CMS muon trigger

The CMS trigger[12] consists of two physical levels: a Level-1 (L1) trigger and a High-Level Trigger (HLT). The p_{T} thresholds of muons at L1 and HLT in the default settings are listed in Table 1. Thereafter, a low luminosity scenario (2×10^{33} cm$^{-2}\cdot$s^{-1}) is assumed.

Table 1. Trigger conditions in the default settings.

menu item	trigger condition	threshold (low Lumi.)	threshold (high Lumi.)
L1	single muon	p_T >14 GeV/c	p_T >20 GeV/c
L1	di-muon	p_T >3 GeV/c	p_T >5 GeV/c
HLT	single muon	p_T >19 GeV/c	p_T >31 GeV/c
HLT	di-muon	p_T >7 GeV/c	p_T >10 GeV/c

For this B_s event data sample, the trigger efficiencies for single muon and di-muon selection at L1 are shown in Table 2. The "L1 any muon bit" means that this event has either a single muon bit or a di-muon bit.

Table 2. Trigger efficiency.

triggering	efficiency
L1	
L1 single muon bit	8.93%
L1 double muon bit	33.7%
L1 any muon bit	36.7%
L1 decision	36.9%
reconstruction efficiency	
efficiency for events that pass L1 criteria	27.4%
overall efficiency (including L1 decision)	36.9%×27.4%=10.1%

The efficiency is defined as the ratio between the number of events triggered and the number of events generated, i.e. eff $= N_{\text{triggered}}/M_{\text{generated}}$. The L1 decision efficiency is 36.9%. The J/ψ reconstruction efficiency in these events is 27.4%, leading to a final efficiency after the L1 decision of 10.1%.

For each event, the global HLT decision (a boolean) and the detailed response (multi-bits) can be computed for the candidates passing the L1 criteria. The trigger is described by a binary tree made of elements (e.g. single electron, single tau, etc.) and logical nodes (e.g. "and", "or", etc.). It allows for a dynamical trigger definition.

In the CMS reconstruction package ORCA version 8.7.1, the HLT response is packed into a string of 93 bits. In this study, we use a few trigger bits containing details about the single muon and double muon responses (e.g. the trigger "HLTmuons" and "double_muons" described in Table 3).

One thing should be emphasized is that some bits are used to mark the presence of at least one muon available to form a di-muon candidate, but it does not necessarily imply the presence of two muons.

Table 3. The HLT single muon and double muon trigger efficiencies.

HLT trigger response	efficiency
HLTmuons: single L3 Mutrigger	0.20%
double_muons: combinatorial and trigger	0.44%
HLT decision	
either of above two: any muon was triggered	0.63%
HLT global decision (cumulative after L1 and HLT)	0.66%
offline reconstruction	
efficiency (i.e. offline) for events that pass HLT	68%
overall efficiency (L1×HLT×offline)	0.45%=0.66%×68%
mass resolution for J/ψ's that passed HLT	0.96%

From Table 3, it can be seen that the HLT decision efficiency is 0.66% w.r.t. generated events, and the J/ψ reconstruction efficiency in these events passing the HLT selection (i.e. two reconstructed muons with an invariant mass in a 3σ window around the J/ψ mass) is 68%. The overall J/ψ efficiency after HLT decision is 0.66%×68%=0.45%. All other efficiencies are cumulative w.r.t. the generated events.

The HLT single muon trigger selects events under the conditions as shown in Table 4. The HLT combinatorial di-muon criteria are similar to the ones employed by the single muon trigger; it requires two muons with a lower p_T threshold (7 GeV/c) plus some additional consistency criteria:

1) The two muons should have different charges.

2) The two muons must have pointed to the same vertex in Z within 5 mm.

3) Muon pairs with $\Delta\phi$ <0.05, $\Delta\eta$ <0.01 and Δp_T <0.1 GeV/c are rejected in order to remove fake tracks.

6.2 J/ψ reconstruction after L1 and HLT decisions

Figure 12 shows the p_T and $|\eta|$ distributions of

Table 4. Conditions for the event selection by HLT muon trigger.

	L2 muon candidates	L3 muon candidates
muon reconstructor	L2 muon reconstructor	L3 muon reconstructor
p_T cut (i.e. p_T + shift $\Delta(p_T)$ >19 GeV/c)	> 19 GeV/c, shift = 3.9	> 19 GeV/c, shift = 2.2
η cut	< 2.5	< 2.5
hits cut	> 3	> 5
isolation cut	calorimeter isolation<0.97	tracker isolation<0.97
vertex cut	check vertex	$(x^2+y^2)^{1/2}$ <0.02 cm

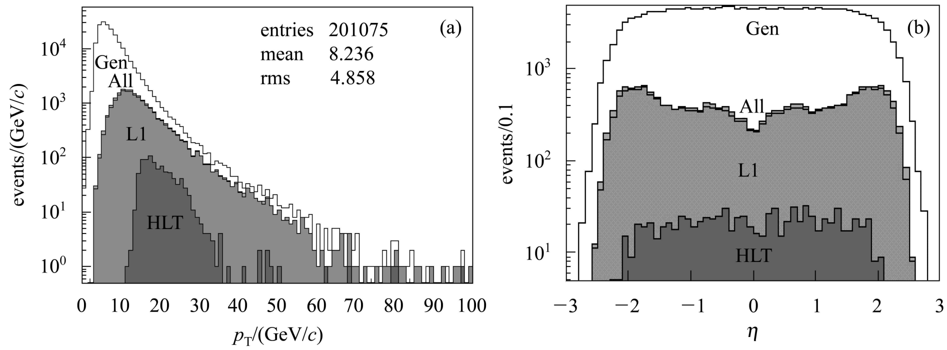

Fig. 12. (a) p_{T} and (b) η distributions of J/ψ candidates at different trigger levels.

J/ψ candidates (i.e. of all possible di-muon pairs within the mass window between 2.95 and 3.25 GeV/c^2) at the generator level and at the reconstruction level, for different trigger requirements.

In Fig. 12, the area "Gen" (white) is for the J/ψ candidates at generator level, the area "All" (light grey) for the J/ψ reconstructed in all events, the area "L1" (darker grey) for the J/ψ reconstructed from the events passing the L1 decision, and the area "HLT" (darkest grey) for the J/ψ reconstructed from the events passing the HLT selection. The J/ψ acceptance after L1 decision is 10.1% as shown in the last line of Table 2, so that the area "L1" is about 10% of the area "Gen". Similarly, the area "HLT" is about 0.5% of the area "Gen", which is consistent with the overall efficiency quoted in Table 3.

From the above tables and plots, it can be seen that the L1 decision saves most of the reconstructed J/ψ events. But after the default HLT decision, most of the surviving J/ψ candidates are in the region 14 GeV/c < p_{T} <30 GeV/c, $|\eta|$ <2.0. In particular, almost all J/ψ candidates with p_{T} >35 GeV/c are rejected after the HLT decision. In order to understand these rejections, we select events with high-p_{T} J/ψ candidates (p_{T} >35 GeV/c). After reconstruction, 338 high-p_{T} J/ψ events are found to have both muons with p_{T} >7 GeV/c, the HLT di-muon threshold.

To understand the HLT inefficiency, we checked the muon separation angle ΔR, defined as $\Delta R = (\Delta\eta^2 + \Delta\phi^2)^{1/2}$, where $\Delta\eta = \eta_{\mathrm{muon1}} - \eta_{\mathrm{muon2}}$ and $\Delta\phi = \phi_{\mathrm{muon1}} - \phi_{\mathrm{muon2}}$. Fig. 13 shows the ΔR distributions for di-muons rejected and accepted by the HLT selection.

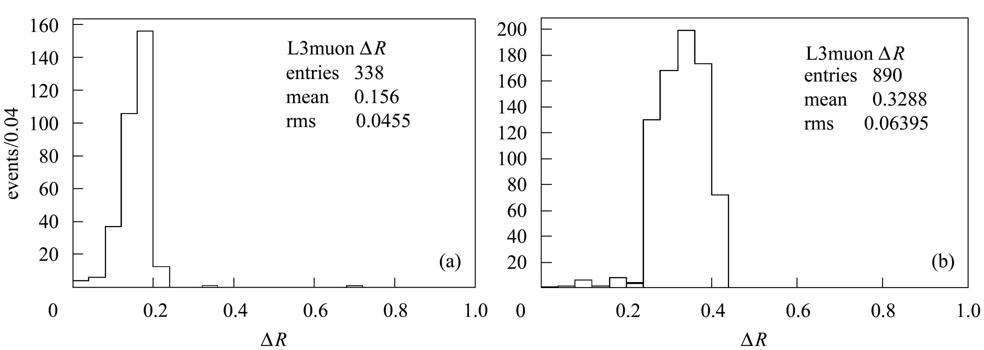

Fig. 13. ΔR distributions for di-muons from high p_{T} (>35 GeV/c) J/ψ for events rejected by HLT (a) and for events passing the HLT selection (b).

From Fig. 13(b), it is evident that most of the di-muons passing the HLT criteria have a large separation angle ΔR (>0.24). In contrast, the di-muons from 338 rejected events have very small ΔR, as shown in Fig. 13(a). In order to understand the origin of this effect, it is important to know the tracker isolation logic used in HLT:

(1) the p_{T} of all charged tracks above some threshold in a cone of ΔR =0.24 around the muon direction are summed up, excluding the the p_{T} of the muon itself;

(2) if the "tracker isolation"[13] variable is larger than 0.97, then this muon is regarded as "being isolated from a jet" and it is accepted by HLT.

Consequently, if a high p_{T} muon is reconstructed inside the ΔR =0.24 cone around another muon, the

HLT isolation criteria will not be satisfied and the event will be rejected. In order to avoid this kind of rejection for high-p_T J/ψ events, the p_T of other muons should not be included when calculating the sum of p_T of nearby particles surrounding one muon.

6.3 J/ψ reconstruction efficiency

The J/ψ efficiencies for different trigger scenarios as a function of p_T are shown in Fig. 14. It can be seen that using the default HLT condition by a simple di-muon cut condition without isolation requirements, the reconstruction efficiency of J/ψ approaches the optimal offline efficiency ("L1"). The default HLT reduces the J/ψ reconstruction efficiency by two orders of magnitude.

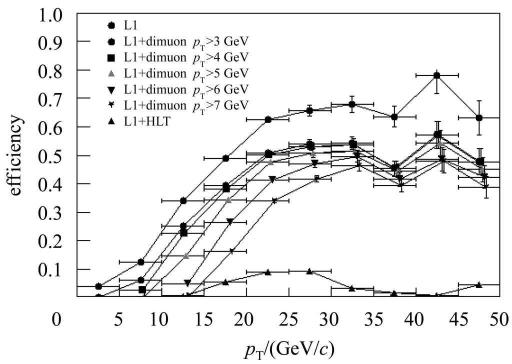

Fig. 14. J/ψ reconstruction efficiency as a function of p_T (for both muons within $|\eta| \leqslant 2.4$).

7 Conclusions

From this study, we conclude that:

(1) The offline reconstruction of $J/\psi \to \mu^+\mu^-$ in CMS reaches an efficiency in the range of 50%—70% for p_T >20 GeV/c. The mass resolution is around 30 MeV/c^2.

(2) The di-muon reconstruction efficiency (i.e. the J/ψ reconstruction efficiency) has some dependence upon the separation angle between two decay muons. It is lower (by about 20%) for small and large separation angles. Small angles happen mainly in the endcap region; large separation angles imply muons with low p_T.

(3) With the default criteria, the L1 trigger retain most high-p_T J/ψ events, while HLT only accepts 0.66% of the J/ψ events, and rejects most events with high-p_T J/ψ mesons. The reason seems to be that the two muons coming from the high-p_T J/ψ decay have a small separation angle. They are declared to be non-isolated by the HLT algorithms, and then rejected. Therefore, when calculating the tracker isolation by summing the p_T of nearby particles surrounding one muon, the p_T contribution from other muons should not be included. The HLT isolation algorithm has been modified in newer versions of the code to avoid this problem.

(4) In order to preserve the rather high L1 efficiency (especially for high p_T J/ψ), the "standard" HLT condition may have to be modified at the tracker isolation level or/and to be supplemented by an additional J/ψ specialized HLT trigger (using an invariant mass cut, for instance).

We would like to thank U. Gasparini for constantly encouraging us and having given many suggestions at various stages of this study. We are also indebted to M. Zanetti, I. Belotelov and J. Alcaraz for their valuable help during the trigger study, and to N. Neumeister and many colleagues for their illuminating discussion in PRS/μ group meetings. We specially appreciate the great help from N. Amapane on the final overhauling for the text of this paper.

References

1 Evans L, Bryant P (editors). Journal of Instrumentation, 2008, **3**: S08001
2 Chatrchyan S et al. (CMS Collaboration). Journal of Instrumentation, 2008, **3**: S08004
3 Cho P, Leibovich A K. Phys. Rev. D, 1996, **53**: 6203
4 Abe F et al. (CDF Collaboration). Phys. Rev. Letters, 1997, **79**(4): 572
5 Abulencia A et al. (CDF Collaboration). Phys. Rev. Lett., 2007, **99**: 132001
6 Karimaki V et al. CMKIN v3 User's Guide, CMS IN 052, 2004
7 CMS Collaboration. CMS Simulation Software OSCAR. http://cmsdoc.cern.ch/oscar/
8 CMS Collaboration. CMS Reconstruction Software ORCA. http://cmsdoc.cern.ch/orca/
9 Belotelov I, Neumeister N. CMS AN 2005/010, 2005
10 Yang Z, Qian S. CMS NOTE 2007/017, 2007
11 Lagouri T. Atlas-muon-2002-008, 2002
12 CMS Collaboration. CMS Trigger Technical Design Report, CERN/LHCC 2000-38, 2000
13 CMS Collaboration. CMS Physics Technical Design Report (Volume 1), CERN/LHCC 2006-001, 2006